Evaluation and Design of Wind Vanes

J. WIERINGA

Royal Netherlands Meteorological Institute, De Bilt

(Manuscript received 12 May 1967, in revised form 23 August 1967)

ABSTRACT

Wind vane motion constants (damping ratio, natural wavelength and decay distance) are derived in a way which can accomodate both mechanical friction and the presence of a propeller. The motion is shown to be insufficiently described by a second order equation because of the way in which the aerodynamic torque changes with angle of attack. This implies that any measurements of vane constants made in the wind tunnel at initial angles of attack above 20° are not representative for the vane. Simple relations between easily measured vane dimensions and motion constants are derived, and vane motion is proved to be independent of the fin area.

The WMO requirement for wind vanes is translated into motion constants and shown to be fulfilled for any vane with a damping ratio of 0.30. For turbulence measurements a certain short-wavelength reliability limit for vane-measured spectra is proposed. Experimental comparison of basic fin configurations shows the inferiority of streamlined and splayed fins.

General vane design rules are given and are applied in the construction of an operational wind vane with a damping ratio of 0.30 and of a fast propeller bivane with an annular fin.

1. Introduction

The motion of wind vanes can be described, as Arakawa (1931) and Giblett (1932) first discovered, by a differential equation of the second order. All investigations on the influence of the vane fin shape on this motion have been conducted either through the use of a constant lift curve slope (Garbell, 1947; Barthelt and Ruppersberg, 1957; MacCready and Jex, 1964) or through flow potential calculations as given by Sanuki (1950).

In this paper a reappraisal of the actual form of the vane motion equation, as determined by the vane construction and fin shape, leads to simplified equations for characteristic motion parameters. These equations can be adapted to accomodate mechanical friction and the presence of a propeller, and lend themselves readily for graphical use. An experimental comparison of several basic vane blade shapes is given, with special reference to the requirements for the proper conduct of wind vane tests. A discussion of optimal vane design is given.

2. Fin aerodynamics

The fin of a simple wind vane, as depicted in Fig. 1a, can be regarded as an airfoil with span b, chord c and area S, with an angle of attack β between the vane axis and the wind u. The shape of the area, including backsweep, is generally accounted for by its aspect ratio $A=b^2/S$ and its edge correction E, equal to the ratio of the semi-perimeter to the wing span. All quantities in this paper will be expressed in mks units, and angles are given in radians unless otherwise indicated.

A dynamic wind pressure $q=0.5\rho u^2$, where ρ is air density, will result in a β-dependent static force F applied at the aerodynamic center, which for any airfoil lies at approximately $\frac{1}{4}c$ from the leading edge. The distance between this $\frac{1}{4}c$-line and the vane pivot is r_v, where the distance between pivot and counterweight centroid is r_w (see Fig. 1a). Components of F are normalized into force coefficients through division by qS, where S is the airfoil projection in the plane of zero angle of attack. Airfoil behavior usually is specified by means of one component perpendicular to u, through the lift force coefficient $c_L=F_L/qS$, and one component parallel to u, through the drag force coefficient $c_D=F_D/qS$. In the case of vane fins c_D is about one order of magnitude smaller than c_L. The dependence of c_L on foil shape, is according to Pope (1951), well approximated by

$$c_L=\frac{c_{L0}A}{AE+2}, \tag{1}$$

where c_{L0} is the value of c_L for infinite aspect ratio.

In the case of vane motion the effective force component F_v will be directed perpendicular to the vane arm; its force coefficient c_v will be equal to c_L only for single-fin vanes at small deflection angles. Fig. 1c shows the situation for vane blades placed at an angle ϕ to the vane arm and having an effective angle of attack $\alpha=\beta-\phi$. If c_L and c_D are known as functions of α,

trigonometrical evaluation of Fig. 1c will show that

$$\frac{F_v}{qS}\equiv c_v(\beta)=c_L(\alpha)\sec\left[\arctan\left|\frac{c_D(\alpha)}{c_L(\alpha)}\right|\right]\times\cos\left[\arctan\left|\frac{c_D(\alpha)}{c_L(\alpha)}\right|-\beta\right]. \quad (2)$$

For a double-fin vane without much interference between the fins, c_v follows from addition of the c_v-values for the separate fins, with due attention to the sign and to the doubling of S. Thus, for a symmetrical vane c_v will always be zero at $\beta=0$, so that "preload" (Garbell, 1947) does not exist. Insofar as the c_v-values of the separate fins are not zero at $\beta=0$, the only effect is a strain on the construction.

The calculated c_v (β), resulting from experimental determination of c_L and c_D, includes all static stalling effects which may occur. The appearance of stalling makes the application of potential theory unsuitable for wind vane evaluation. To give an example, according to potential theory, the Duplex Anemovane (Sanuki, 1950) was designed for optimal performance with two curved airfoils at $\phi=-20°$; actually, it proved to have off-center equilibrium. Calculation of c_v (see Section 4) shows that for this case negative c_v-values are found for $\beta<11°$, resulting in an *outward* force at $\beta=0$. On checking this surprising result with a model vane in the Royal Netherlands Meteorological Institute (KNMI) wind tunnel, two equilibrium points with a relative distance of 15° were found, with the tunnel direction in between; the effect appeared clearly at high tunnel speeds and thus is not due to friction errors. The actual extent of the "forbidden sector" seems to be larger when r_v is small with regard to the relative distance of the blades. Experiments with other model vanes also indicate a dependence of the forbidden-sector effect on wind speed in a rather unsystematic fashion, the double stability either increasing or decreasing with u for different configurations with the same value of ϕ. More extensive research will be described in a KNMI report to be published by the author in 1968.

Two operational vanes with a forbidden sector have been described by Noetzlin (1941). One of these useless contraptions, the Lambrecht 1465, is still offered for sale.

3. Vane motion equation

a. General derivation and characteristic parameters. The effective force F_v on a vane fin produces for unit angle of attack a torque

$$N\equiv r_vF_v/\beta. \quad (3)$$

For a moving vane (see Fig. 1b) a supplementary force results from the fin speed $r_v\dot{\beta}$ (where $\dot{\beta}\equiv d\beta/dt$), which changes the effective angle of attack β_v and the effective

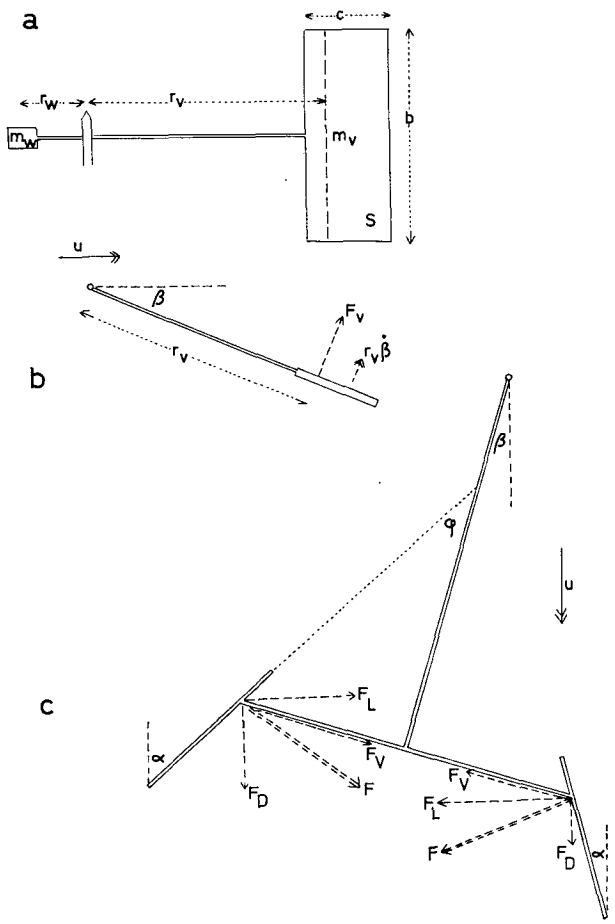

FIG. 1. Statical vane description; a., side view; b., plane view; c., forces on double-fin vane.

wind speed u_v acting on the fin. Barthelt and Ruppersberg (1957) have shown that $u_v\approx u$ for actual vane motion, and that

$$\beta_v=\arctan\left(\frac{u\sin\beta+r_v\dot{\beta}}{u\cos\beta}\right)\approx\beta+\frac{r_v\dot{\beta}}{u}, \quad (4)$$

the latter approximation being valid for not too large values of β. Then for a vane with moment of inertia J, the equilibrium condition is

$$-J\ddot{\beta}=r_vF_v=N\beta_v=N\beta+\left(\frac{r_v.N}{u}\right)\beta, \quad (5)$$

where

$$\frac{r_v.N}{u}\equiv D \quad (6)$$

is the aerodynamic damping of the vane. Any mechanical friction will result in the addition of an extra damping term $D_m\dot{\beta}$; this will be considered later on in this section.

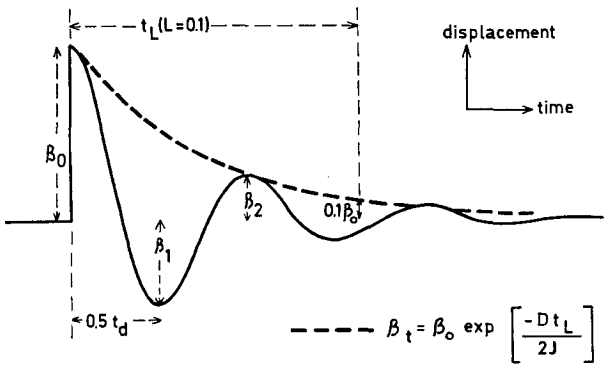

FIG. 2. Response of vane with $h=0.5$ to step displacement.

If N is constant, the second order equation (5) has the solution

$$\beta=\beta_0 \exp\left(\frac{-D}{2J}t-2\pi i\frac{t}{t_d}\right), \tag{7}$$

where β_0 is the initial displacement and

$$t_d=2\pi\Big/\left[\left(\frac{N}{J}\right)-\left(\frac{D}{2J}\right)^2\right]^{\frac{1}{2}} \tag{8}$$

is the damped oscillation period of the vane. For an undamped vane this reduces to the natural oscillation period,

$$t_0=2\pi\Big/\left(\frac{N}{J}\right)^{\frac{1}{2}}. \tag{9}$$

The critical damping D_0 of the vane is defined by

$$\frac{N}{J}=\left(\frac{D_0}{2J}\right)^2, \tag{10}$$

while the actual damping of the vane is usually specified by the damping ratio

$$\zeta\equiv D/D_0=r_vN/uD_0. \tag{11}$$

Substitution of (9) and (10) reduces (11) to

$$\zeta=\pi r_v/ut_0. \tag{12}$$

Vanes are generally subcritically damped ($\zeta<1$) and oscillate, so as to be able to reach zero deflection within a finite period.

The real part of (7), exp $(-Dt/2J)$, describes the envelope of the damped oscillation executed by the vane after release from an initial step displacement angle β_0 (see Fig. 1d). After a time t_L the position error β resulting from the step displacement will be at most $\beta_t=\beta_0$ exp $(-Dt_L/2J)$ and probably less. We call $\beta_t/\beta_0\equiv L$ the decay fraction remaining of the initial displacement after a decay time

$$t_L=\frac{-\ln L}{D/2J}=\frac{4.61\log(1/L)Ju}{r_vN}. \tag{13}$$

This is illustrated in Fig. 2 for $L=0.1$.

The above calculations require N to be constant. Substitution of $\rho=1.25$ kg m^{-3} (for sea level) in (3) gives

$$N=0.625\,u^2r_vS\,c_v/\beta. \tag{14}$$

For a specified vane construction in a specified wind this defines the torque parameter $a_v\equiv c_v/\beta$, accounting for the influence of fin shape on vane motion. The value of a_v will be determined experimentally in Section 4.

Without explicitly stated justifications Garbell (1947) and subsequent authors employ a dynamic parameter, the torque curve slope $dN/d\beta$ in the static equilibrium equation. In the case of an ordinary flat vane fin the resulting error is only slight if the motion is restricted to $\beta<10°$, because then both c_v/β and $dc_v/d\beta$ are constant, have the same order of magintude, and depend in the same way on A and E. But for large angles of attack the use of $dN/d\beta$ produces errors; for example, $dc_v/d\beta$ is zero at $\beta=90°$, while the vane torque is certainly not zero when the vane is perpendicular to the wind.

Substituting (14) in (9), (12) and (13), we obtain the following relations (derived in a different fashion by other authors):

$$ut_0=7.95\left(\frac{J}{a_vr_vS}\right)^{\frac{1}{2}}, \tag{15}$$

$$\zeta=0.395\left(\frac{a_vr_v{}^3S}{J}\right)^{\frac{1}{2}}, \tag{16}$$

$$ut_L=\frac{7.37\log(1/L)J}{a_vr_v{}^2S}. \tag{17}$$

Since all the factors on the right-hand side of these relations are constant for a specified vane, the quantities ut_0 ("natural wavelength"), ζ ("damping ratio") and ut_L ("decay distance") can be regarded as constant characteristic parameters of the vane motion. The parameters ut_0 and ut_L have length dimensions, while ζ is dimensionless. Only two of these need to be known to specify fully the motion properties of a vane.

Two alternative parameters, also being constant for a given vane, are of considerable practical use. From (8) one can show that

$$ut_d=ut_0/(1-\zeta^2)^{\frac{1}{2}}. \tag{18}$$

This damped wavelength is the distance travelled by the wind between two positive (or negative) peaks of the vane oscillation, as illustrated in Fig. 2. The decrease in amplitude between two subsequent extremes can be

shown from (13) to be

$$h \equiv \beta_i/\beta_{i-1} = \exp\left(\frac{-Dt_d}{4J}\right) = \exp\left(\frac{-\pi\zeta}{(1-\zeta^2)^{\frac{1}{2}}}\right), \quad (19)$$

and is called the overshoot fraction (see Fig. 2).

Another frequently employed parameter, the "delay distance," defined as the distance after which the initial displacement is halved for the first time (MacCready and Jex, 1964), is of little practical use for any vane with $h>0.5$, and is also rather difficult to measure with any precision.

b. Propellers and other forward surfaces. For vanes with a non-negligible forward surface, e.g., a non-moving propeller, the given derivation can be easily modified. If the forward surface projection perpendicular to the vane motion S_w is at an effective distance r_w from the pivot and if it has a torque parameter a_w, the resulting unit torque will be $N_w=0.625\ u^2 r_w S_w a_w$. Because r_w is negative, N_w must be subtracted from the main blade torque N to obtain the total restoring torque $N_T=N-N_w$. On the other hand (6) contains r^2, and thus the total aerodynamic damping D_T is the sum of two separate aerodynamic dampings, i.e.,

$$D_T=(r_v N+r_w N_w)/u.$$

Recalculation with N_T and D_T results in:

$$ut_0=7.95\left(\frac{J}{a_v r_v S-a_w r_w S_w}\right)^{\frac{1}{2}}, \quad (20)$$

$$\zeta=\frac{a_v r_v^2 S+a_w r_w^2 S_w}{2\left(\frac{J}{a_v r_v S-a_w r_w S_w}\right)^{\frac{1}{2}}}, \quad (21)$$

$$ut_L=\frac{7.37\log(1/L)J}{a_v r_v^2 S+a_w r_w^2 S_w}. \quad (22)$$

Propeller motion cannot be incorporated within the limits of this derivation. Later on in this paper it will be shown from experimental results that the influence of propeller rotation is small, but not negligible.

c. Area elimination. For an average wind vane, as illustrated in Fig. 1a, the moment of inertia can be sufficiently well approximated by restricting the calculation to the effects of the fin mass m_v and the counterweight mass m_w. Even when the fin centroid is taken at a distance r_v from the pivot, i.e., $\frac{1}{4}c$ too close, the error is as a rule far less than 1%, even for vanes of heavy construction.

Taking into account that the vane must balance about its pivot ($m_v r_v=m_w r_w$), we obtain

$$J\approx m_v r_v^2+m_w r_w^2=m_v r_v^2(1+r_w/r_v). \quad (23)$$

Define the weight of a unit fin area $\mu_v \equiv m_v/S$ and a vane quality factor

$$K_v \equiv a_v/\mu_v(1+r_w/r_v). \quad (24)$$

Then

$$J\approx a_v S r_v^2/K_v. \quad (25)$$

Substitution of (25) in (15), (16) and (17) results in:

$$ut_0=7.95\left(\frac{r_v}{K_v}\right)^{\frac{1}{2}}, \quad (26)$$

$$\zeta=0.395(r_v K_v)^{\frac{1}{2}}, \quad (27)$$

$$ut_L=\frac{7.37\log(1/L)}{K_v}. \quad (28)$$

Since μ_v pertains to unit area only, the fin area S thus is of no importance towards the motion of a frictionless wind vane. For propeller vanes with their rather complex build-up of masses, it will be more correct to calculate with J, because (23) is not valid there. Even so, K_v can be determined from (25) if J is known, and all conclusions remain valid.

The relations (26), (27) and (28) are suitable for simple graphic illustration for purposes of design or comparison. This has been done in Fig. 3.

d. Criteria of vane usefulness. The decay distance ut_L is a useful quantity in determining the minimum distance travelled by the wind after which vane oscilla-

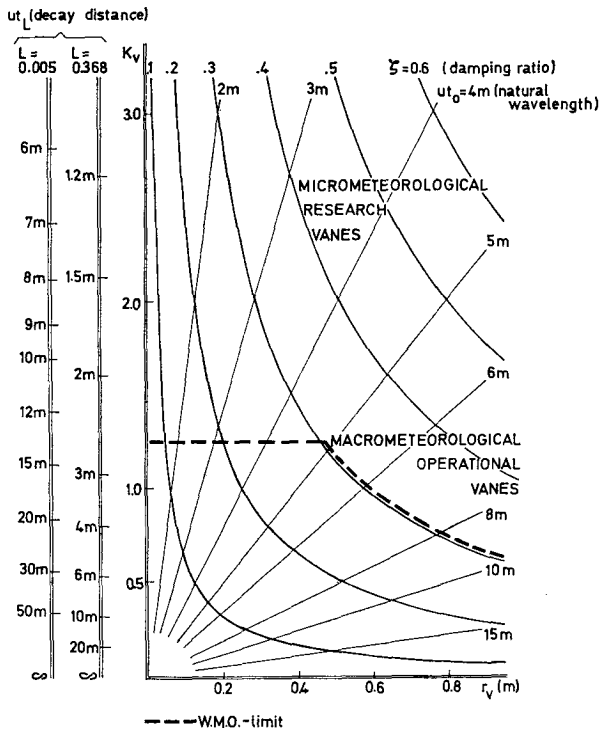

FIG. 3. General relations of vane parameters.

tions can be disregarded down to a predetermined error limit. The practical choice of the decay fraction L is to a certain extent arbitrary, and variation of L only amounts to a different scale along the K_v-axis. Another advantage of ut_L is the possibility to consider it as analogous to the lag-distance concept found in first-order systems like propellers.

Official W.M.O. regulations (WMO-No. 8 TP. 3, 6.2.3) request that a vane approaches zero position within 37% after 1 sec when $u=5$ kt. The decay fraction, $L=1/e=0.368$, was also used by Sanuki, Kimura and co-workers in a series of investigations from 1955 onwards (Sanuki *et al.*, 1955). For $L=0.368$ we obtain $ut_L=3.20/K_v$ from (28). The WMO limit then follows from $ut_L=5\times0.515$ m, so that $K_v=1.25$. But it can also be shown that the WMO request is complied with for vanes with $h\leqq0.37$ ($\zeta>0.30$) and $r_v<1.92$ m. The composite WMO-limit is drawn in Fig. 3; to my knowledge at the present moment not a single vane in the world used for macrometeorological measurements complies with the WMO request.

A second choice of C follows from micrometeorological considerations. To determine the high frequency limit for turbulent fluctuation measurements for the MIT bivane as described by Cramer *et al.* (1961), Kaimal *et al.* (1964) have compared it with a sonic anemometer. They found that coherency of the spectrum disappeared altogether for fluctuations with a wavelength below 10 m; thus, at that point random oscillations of the vane, however small, interfered destructively with the actual small fluctuations to be measured. An approximate evaluation of the MIT bivane from Cramer *et al.*, gives $K_v\approx1.75$, corresponding with a decay fraction following from

$$ut_L=10\text{ m}=\frac{7.37\log(1/L)}{1.75}.$$

The nearest round figure for L is 0.005, giving $ut_L=17.0/K_v$. This choice of decay distance seems suitable as a rough indication of the minimal fluctuation dimension which can be accurately measured by a pure wind direction sensor like the MIT-bivane, furnished with a hot-wire anemometer capable of high-frequency measurements.

A vane having an effective length r_v which is too large to be neglected in comparison with the decay distance ($L=0.005$) will, of course, introduce an extra geometric error in the measurement of small fluctuation dimensions. Such a long vane will also have a large damped wavelength ut_d, and if ut_d is larger than the decay distance, one might consider the latter to be no longer a true measure of the vane sensibility. The limit of the usefulness of ut_L ($L=0.005$) as a criterion for the smallest spectral wavelength which is measured accurately will therefore be defined by

$$ut_L\left(=\frac{17.0}{K_v}\right)=ut_d\left[=\frac{7.95}{(1-\zeta^2)^{\frac{1}{2}}}\left(\frac{r_v}{K_v}\right)^{\frac{1}{2}}\right],$$

from which it follows that $\zeta=0.65$. This ζ-curve (not drawn in Fig. 3) might be considered as an effective limitation on the right-hand side of the ut_L ($L=0.005$) isolines, or as an indication of the largest r_v-value which can be usefully combined with a specified K_v-value. It also appears that it does not pay, dynamically, to increase the damping too far towards the critical damping D_0.

For a vane with a slowly adjusting velocity sensor, like a propeller, the response distance L_p of this sensor should also be taken into account when determining a high-frequency limit for fluctuations measurements. If the velocity sensor lag should not influence measurements of fluctuation dimensions of the same order of magnitude as ut_L ($L=0.005$), it appears desirable that the velocity measurement error should also be 0.5% or less. When the response distance L_p of the velocity sensor is defined to be the product of the mean wind velocity and the period after which the velocity measurement is adjusted to a sudden change within 36.8% (MacCready and Jex, 1964), then a 0.5% error will be attained when $\exp(-X/L_p)=0.005$, that is at a distance $X=5.3\ L_p$. For measurement of fluctuation dimensions larger than both ut_L ($L=0.005$) and $5.3\ L_p$, it also seems safe to neglect to a first approximation any phase mismatch errors due to the distance between propeller and vane blade.

The considerations given above explain the designation of certain regions of r_v-K_v values in Fig. 3 as optimal for vanes designed for micrometeorological or macrometeorological measurements.

e. Effects of mechanical friction. As mentioned before, mechanical friction will increase the damping term in (5) by a term $D_m\dot{\beta}$. Recalculation of (18), (27) and (28) with this damping results in:

$$ut_d\approx\frac{7.95(r_v/K_v)^{\frac{1}{2}}}{(1-\zeta^2-r_vD_m/u)^{\frac{1}{2}}},\tag{29}$$

$$\zeta=0.395(r_vK_v)^{\frac{1}{2}}+\frac{0.63D_mK_v^{\frac{1}{2}}}{ua_vSr_v^{\frac{3}{2}}},\tag{30}$$

$$ut_L=\frac{7.37\log(1/L)}{K_v[1+0.22D_m/(ua_vSr_v^2)]}.\tag{31}$$

The net effect of mechanical friction is generally a sizeable increase of ζ, a moderate increase of ut_d and a small decrease of ut_L. In the r_v-K_v graph this signifies a displacement towards larger r_v values, while the displacement towards larger K_v values will be rather small. The mechanical friction effect decreases with

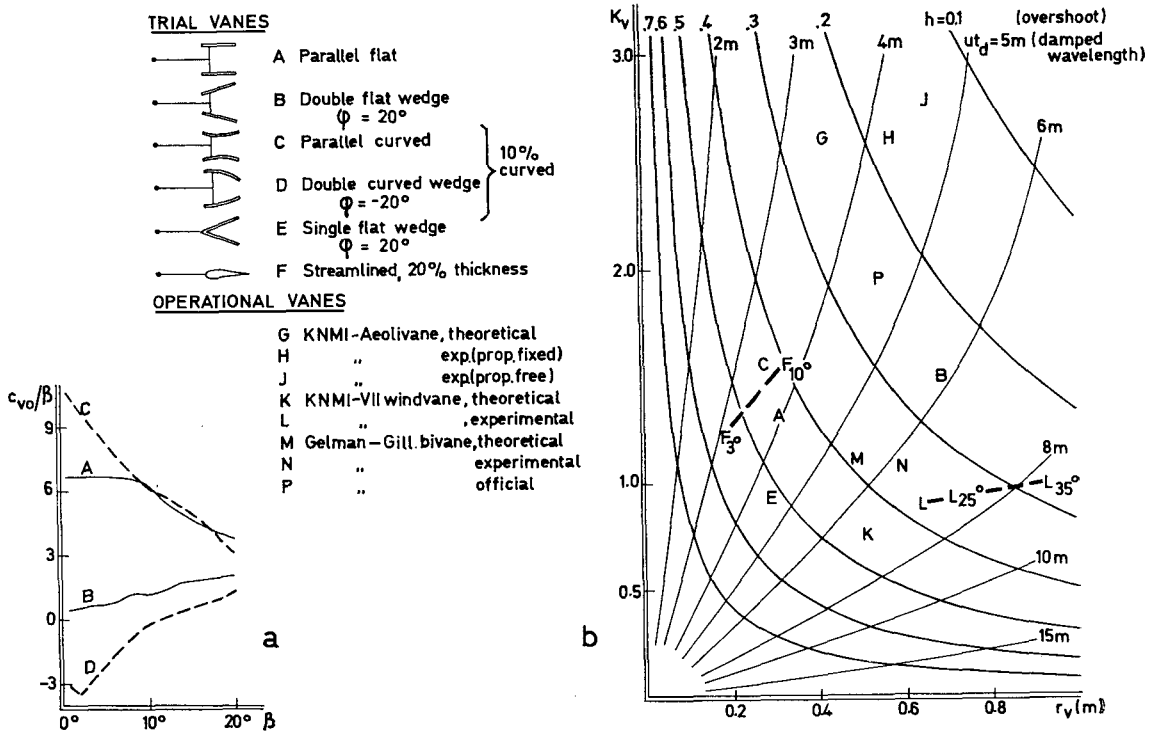

FIG. 4. Vane and fin comparison: a., torque parameter; b., experimental results.

increasing wind speed; this means that a vane, which relies on friction to obtain a ostensibly large damping, will behave badly in strong winds. Any additional non-aerodynamical damping should thus be velocity-dependent to be fully effective; for instance, Sanuki *et al.* (1965) use oil-damping, and magnetic damping with anemometer input might also be used.

4. Fin type comparison

For some basic fin configurations, which consist of independent flat or 10% curved plates, a_v can be calculated according to (2) and is given in Fig. 4a. The values of c_L and c_D were taken from Flachsbart (1932), and the results corrected according to (1) to obtain c_{v0}/β for infinite aspect ratio. The negative values occurring for 10% curved fins with $\phi = 20°$ have already been discussed.

Various authors have postulated that a $\cos^2\beta$ factor should be included in any expression for fin action so as to account for changes in the angle of attack, because the size of a projection on a plane stationary with respect to the wind direction follows a $\cos\beta$ relationship, and the dependence of aerodynamic force on angle of attack is erroneously postulated to be a pure $\cos\beta$ relationship. In the present approach, however, it follows from the definitions in Section 2 that the use of c_v implies reference to a *constant* area, the projection of the fin (or fins) on the $(\beta=0)$-plane of the vane, which plane is stationary with reference to the vane itself. All angle-of-attack effects are thereafter implied in the $a_v(\beta)$ function.

From experimental data the a_v-curves of Fig. 4a have been derived, and they bear not the slightest resemblance to $\cos\beta$-function curves; only for curve A (flat-plate fin) is a rough $\cos\beta$-approximation possible if the stalling dip around 11° is neglected.

The general impression of Fig. 4a is that a_v is only constant for simple flat-plate fins at $\beta<10°$, and that for other fin configurations the static torque changes in a way peculiar to each configuration. The influence of a change of torque on vane motion, however, cannot easily be determined by mathematical means, for even the substitution of the simple approximation, $N=N_0 \times(1+K\beta)$, in (5) will render this equation insoluble in terms of elementary functions.

Even though the description of vane motion as a second-order system thus appears to be not quite correct, it is still useful to retain the description by the second-order parameters described above. An experimental approach was therefore used to determine the effective torque parameter a_{ve} for various fin configurations from their motion parameters. For this purpose a trial vane with exchangeable fins was used. The specifications for all experiments were that $\mu_v=1.48$ kg m^{-2}, $r_v=0.23$ m, $r_w/r_v=0.28$, relative distance of double fins $=2.4\,c$, and $A/(EA+2)=0.545$. The results of step function measurements in the KNMI-wind tunnel are given in Fig. 4b, a graph with isolines of the experimental parameters ut_d and h.

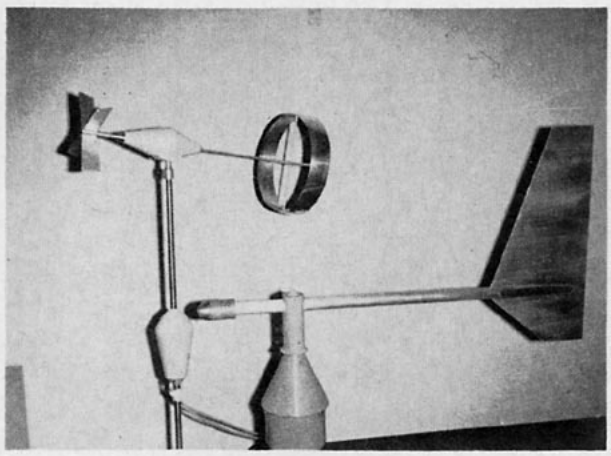

FIG. 5. KNMI Aeolivane and KMNI-VII wind vane.

The first conclusion is that the observed K_v-values for different fins are much closer together than their respective a_v-values. Thus, it can be concluded from comparison with the flat fin (A), that for the double wedge fin (B) the increase of a_v with β seems to compensate the relatively low value of a_v; similarly, the parallel curved fin vane (C), combining a relatively high a_v-value with a negative a_v-slope, obtains about the same magnitude of effective K_v as the flat fin.

Practical comparison of (A), (B) and (C) with regard to dynamical behavior shows that they are roughly equivalent with respect to decay distance, and that (B) will have less overshoot than either (C) or (A). Good response at low wind speeds is a statical quality depending on the torque value only, so in this respect (B) will be inferior to (A) and (C).

The second conclusion is that the single wedge fin (E) and the streamlined fin (F) are decidedly inferior to the simple flat fin in all respects, notwithstanding their popularity due to vague intuitive reasoning (Grunow, 1935). For the streamlined fin the relatively bad characteristics for small angles of attack were to be expected, because a good streamline is meant to diminish aerodynamic action. For the single wedge, also called "splayed fin," the fin plates apparently diminish each other's effectiveness.

For purpose of theoretical evaluation of dynamical behavior for the "good" fin types (A), (B) and (C), the effective torque parameter follows from their rough average $K_v=1.4$ and the trial vane specifications. Using (24) and (1) it follows that $a_{ve}=4.9$ for infinite aspect ratio. For blades of specified dimensions then

$$a_{ve}=4.9A/(EA+2). \tag{32}$$

5. Vane design considerations.

It has been shown above that for optimal vane performance the vane quality factor,

$$K_v=a_{ve}/[\mu_v(1+r_w/r_v)],$$

must be high. From (32) follows the desirability of the largest aspect ratio which the stiffness of the fin construction will tolerate.

The presence of the factor $1/(1+r_w/r_v)$ and the absence of m_w in K_v means that a heavy counterweight on a short arm must be used. The omission of the counterweight gives great operational difficulties, and the improvement of K_v is only 10% compared with the case that $r_w=0.11\ r_v$. Those who are preoccupied with lightness of vane construction often employ a light counterweight on a long arm (Sanuki *et al.*, 1966), apparently not realizing that thus they obtain a relatively large moment of inertia.

Though it might seem advantageous according to Section 3b to shape the counterweight in such a fashion that the side surface is as large as possible, this is actually not worth the trouble because for a small r_w-value the effectiveness of such a small frontal surface is negligible.

The employment of double-faced aerodynamic profiles seems to be of doubtful use, since the increase in μ_v relative to a single-plate profile will not sufficiently be compensated by the increase of a_v. For the symmetrical profile (F) this has been shown above. Asymmetrical profiles of the Joukowski type generally have poor lift in the direction which an aeroplane should not take to avoid disaster; and since two profiles are needed to construct a symmetrical vane, the net c_v-value will at most equal c_v for a flat plate. The possibility of employing Joukowski profiles in bivanes through the use of annular fins, as suggested by Garbell (1947), is thus no justification for embarking upon ring-shaped constructions.

For the single-plate types (A), (B) and (C) mentioned in Section 4, their response at low wind speeds depends on a_v, r_vS and the choice of bearings, and is therefore the only vane property which is a function of fin area. When calculating the unit fin area weight, $\mu_v=m_v/S$, the area S to be considered is the fin projection onto the $\beta=0$ plane of the vane, chosen appropriate for the angular motion considered. This means that for the conventional crossed-plane bivane of the MIT type, μ_v will be twice the value found for a single vane having the same weight per area construction surface, because the single vane (for horizontal motion) does not suffer the inertia of an ineffective horizontal fin. In this respect the optimal construction for a bivane fin seems to be a ring shape, which has a relative weight increase factor of only 1.57 compared with a single blade. The added weight of the ring supports is compensated in practice because the annular construction allows a high aspect ratio (and $E=1$) to be combined with a reasonable stiffness; the aspect ratio in this case is calculated as ring diameter/ring chord. The agreement found for the Aeolivane, described below, between the K_v-value calculated in the above manner ($K_v=2.60$) and the value found in wind tunnel experiments with non-rotating propeller

($K_v=2.6$) does not exactly invalidate the described calculation methods.

New vane designs. For all-weather micrometeorological measurements at the Royal Netherlands Meteorological Institute, a propeller bivane ("trivane") with a 0.2-mm Al annular fin, the Aeolivane, was designed (see Fig. 5). A large operational wind vane, the KNMI-VII with a 1.0-mm Al fin was also designed to meet the WMO requirements. For both vanes the theoretically calculated parameters (points G and K) and the results obtained from wind-tunnel tests are given in Fig. 4b and are specified below.[1]

The experimental results appear to be consistent with the calculations, the displacement of the parameter points towards (H) and (L) with larger r_v-values being due to the mechanical friction which, being unknown, could not be included in the calculation. The difference between the points (H), Aeolivane with fixed propeller, and (J), Aeolivane with free rotating propeller, shows the unknown gyroscopic influence of the propeller to be a small, but not negligible, increase of ζ and ut_d.

6. Evaluation of wind-tunnel tests on vanes

Having discovered that the wind vane is not a pure second-order system, one would not be surprised if the vane properties depended on the value of β and this is indeed the case: the values of ζ and ut_d change significantly when the initial value of β is large. For a number of vanes with flat fins, having widely different dimensions, the experiments showed, for β between 30° and 40°, an average increase of 0.035 for ζ and of 0.7m for ut_d. In Fig. 4b (where all other vanes are specified by their properties in the range $\beta<15°$ which are more or less constant) the observed increase is indicated for β values of 25° and 35° for the KNMI-VII vane, which from $\beta\approx17°$ onwards starts to change properties. Incidentally, the average registration of the MIT bivane reproduced by Cramer *et al.* (1961) shows the same effect, i.e., $\beta_1/\beta_0=0.28$ and $\beta_2/\beta_1=0.48$.

Investigations of this effect require measurements of h and ut_d over the *same* half-cycle, between two subsequent amplitude peaks of opposite sign. The KNMI experiments were done in a large wind tunnel with a fast Servogor recorder; after calculating the highest possible $d\beta/dt$ value from (7), the angle amplification of the recorder was set at a value small enough to guarantee faithful registration.

The observation, not only for flat fins of type (A), but also for curved parallel fins of type (C), that the increase of ζ and ut_d begins rather abruptly around $\beta\approx15°$ would seem to indicate that the dynamic consequences of the stalling of the vane blades are the cause of this increase, and not the behavior of the static parameter a_v. This explanation would also cover the behavior of (B)-type fins, with $\phi=20°$, for which both fins are stalled for $\beta<5°$ and $\beta>35°$, while for $5°<\beta<35°$ one of the fins permits smooth air flow. For these double wedge vanes, experiments show between $\beta\approx10°$ and $\beta\approx30°$ a decrease in damping ratio for increasing β, ut_d remaining constant, and after $\beta\approx30°$, an increase in ζ and ut_d.

Test requirements. For meteorological practice in which wind direction changes, however sudden, will never be instantaneous, the actually occurring values of β will be small and usually within the range $\beta<15°$. To measure faithfully the vane parameters for this range of angles it will not do to disregard the dependence of the vane parameters on β shown above. Having obtained a wind-tunnel step function registration in the manner detailed by MacCready and Jex (1964), the incorrect way to evaluate it will be to obtain h from the largest peaks, which are easily measured, and ut_d from the distance between two zero crossings separated by a full cycle; in the latter measurement the large initial value β_0, which was used to determine h, will not play a part and thus small angles will predominate in the ut_d-evaluation. Thus, we obtain a more or less correct value for ut_d, but a much too large value for ζ. Use of a slow recorder will, of course, give an additional increase of apparent damping for large initial deflections.

For the reasons outlined above any official vane specifications given without specification of the β-range should be regarded with caution. Experimental proof of erroneous official specifications was obtained for the Gelman-Gill bivane, for which the official specifications ($\zeta=0.43$, $ut_d=4.6$ m) are represented by (P) in Fig. 4b. Theoretically calculated results based on the vane construction are indicated by (M), and the actual accurate values found from wind-tunnel measurements at $\beta<15°$ are represented by (N). The experimental results appear to be consistent with the calculations, the small displacement towards larger r_v-values being due again to mechanical friction.

In wind-tunnel experiments attention should also be given to the wind speed used. From (29) and (30) it follows that, because of mechanical friction effects, results obtained at speeds below 2 m sec^{-1} will not be representative for high-speed behavior. On the other side, the highest practical measuring speed is determined by the recorder used.

Acknowledgments. Acknowledgment is due to the Director-General of the Koninklijk Nederlands Meteorologisch Instituut, Prof. Dr. W. Bleeker, for his permission to undertake this study. The author also wishes to thank Prof. Dr. F. H. Schmidt for his critical comments, Ir. J. A. van Ghesel Grothe (T. H., Delft) and Drs. C. J. P. van Buijtenen (T.N.O., Rijswijk) for the loan of equipment, Ir. J. H. Rietman and Mr. W.

[1] Specifications of vanes.

1) *Aeolivane.* $A=5.0$, $r_v=0.235$ m, $r_w=0.14$ m; propeller: 0.3 mm Al, $A=4.9$; calculated $K_v=2.60$; experimental results with rotating propeller: $\zeta=0.54$, $ut_d=4.6$ m, $K_v=2.8$.

2) *KNMI-VII.* $A=3.2$, $r_v=0.45$ m, $r_w=0.15$ m; calculated $K_v=0.76$; experimental results: $\zeta=0.30$, $ut_d=7.0$ m, $K_v=0.90$.

The accuracy of the experiments was ±4%. More detailed descriptions will be given in a future KNMI report.

Hovius for their assistance with the wind-tunnel experiments, and Mr. E. P. F. H. Blokhuis with his staff for the construction development of the designed wind vanes.

REFERENCES

Arakawa, H., 1931: On windvane of the R. A. E. pattern. *Geophys. Mag.*, **4**, 53–59.

Barthelt, H. P., and Ruppersberg, G. H., 1957: Die mechanische Windfahne, eine theoretische und experimentelle Untersuchung I. *Beitr. Phys. Atmos.*, **29**, 154–185.

Cramer, H. E., F. A. Record, J. E. Tillman and H. C. Vaughan, 1961: Studies of the spectra of the vertical fluxes of momentum, heat and moisture in the atmospheric boundary layer. Annual Rept., Massachusetts Institute of Technology, Contract DA-36039-SC-80209, 130 pp.

Flachsbart, O., 1932: Messungen an ebenen und gewölbten Platten. *Ergebnisse der Aerodynamischen Versuchsanstalt zu Göttingen IV*, Berlin, Oldenbourg-Verlag, 96–100.

Garbell, M. A., 1947: Fins for aerological instruments. *J. Meteor.*, **4**, 82–91.

Giblett, M. A., 1932: The structure of wind over level country. *Meteor. Office Geophys. Mem.*, **54**, 20–22.

Grunow, J., 1935: Die Windmessung am Boden. *Handbuch der Meteorologischen Instrumente*, Berlin, Springer-Verlag, 331–340.

Kaimal, J. C., H. E. Cramer, F. A. Record, J. E. Tillman, J. A. Businger and M. Miyake, 1964: Comparison of bivane and sonic techniques for measuring the vertical wind component. *Quart. J. Roy. Meteor. Soc.*, **90**, 467–472.

MacCready, P. B., and H. R. Jex, 1964: Response characteristics and meteorological utilization of propeller and vane wind sensors. *J. Appl. Meteor.*, **3**, 182–193.

Noetzlin, U., 1941: Beiträge zur Frage der Windmessung am Boden unter besondere berücksichtigung der Böenmessung. *Reichsamt Wetterd. Wiss. Abhandl.*, **8**, No. 5, 11–22.

Pope, A., 1951: *Basic Wing and Airfoil Theory*. New York, McGraw-Hill, p. 208.

Sanuki, M., 1950: Studies on biplane wind vanes, ventilator tubes and cup anemometers I, II. *Papers Meteor. Geophys. (Tokyo)*, **1**, 31–132 and 227–298.

——, S. Kimura, N. Tsuda and S. Toyama, 1955: Time constants of biplane windvanes I. *Papers Meteor. Geophys. (Tokyo)*, **6**, 244–246.

——, —— and H. Hayashi, 1965: A proposed wind vane with practically no overshoot. *Papers Meteor. Geophys. (Tokyo)*, **16**, 84–89.

——, ——, and ——, 1966: Wind vane with extremely small moment of inertia and its possible application. *Papers Meteor. Geophys. (Tokyo)*, **17**, 46–50.